

Article

Self-Diffusion Coefficients of Components in Liquid Binary Alloys of Noble Metals

Nikolay Dubinin^{1,2,*} and Roman Ryltsev^{1,2} ¹ Institute of Metallurgy of the Ural Branch of the Russian Academy of Sciences, 101 Amundsen St., 620016 Ekaterinburg, Russia² Ural Federal University, 19 Mira St., 620002 Ekaterinburg, Russia

* Correspondence: ned67@mail.ru

Abstract: An accurate determination of transport coefficients in liquids, such as diffusivity, is crucial for studying fundamental chemical processes, for constructing and verifying model theories of liquid, and for the optimization of technological processes. However, a reliable experimental determination of the diffusivity is a difficult and sometimes nearly impossible task. In this regard, the development of model theories that allow calculating characteristics of atomic transport is of special interest. Here, the concentration dependencies of the self-diffusion coefficients of the components in Cu-Ag, Cu-Au, and Ag-Au liquid alloys at $T = 1423\text{ K}$ and $T = 1573\text{ K}$ are calculated in the framework of the linear trajectory approximation in conjunction with the square-well model and the semi-analytical representation of the mean spherical approximation. We reveal that peculiarities in the behavior of the obtained dependencies are related to the peculiarities of the phase diagrams of the alloys under consideration. Additionally, we verify our calculation method on $\text{Al}_{80}\text{-Cu}_{20}$ and $\text{Al}_{80}\text{-Au}_{20}$ liquid alloys. The results obtained are in good agreement with available experimental and molecular-dynamic simulation data. In the cases when the experimental information is not available, the presented results can be considered as predictive to estimate the quantities under consideration approximately.



Citation: Dubinin, N.; Ryltsev, R. Self-Diffusion Coefficients of Components in Liquid Binary Alloys of Noble Metals. *Metals* **2022**, *12*, 2167. <https://doi.org/10.3390/met12122167>

Academic Editor: Gunter Gerbeth

Received: 28 October 2022

Accepted: 13 December 2022

Published: 16 December 2022

Publisher's Note: MDPI stays neutral with regard to jurisdictional claims in published maps and institutional affiliations.



Copyright: © 2022 by the authors. Licensee MDPI, Basel, Switzerland. This article is an open access article distributed under the terms and conditions of the Creative Commons Attribution (CC BY) license (<https://creativecommons.org/licenses/by/4.0/>).

1. Introduction

Diffusion coefficients are relevant quantities for many important processes, in particular for solidification and microstructure formation in alloys. Progress in experimental and computer-simulation techniques during last two decades has stimulated a great interest for researchers in diffusion in liquid binary metal and metal-like alloys in both experimental [1–21] and theoretical [3,5,21–56] areas. However, the liquid binary alloys of noble metals remain, to our knowledge, not studied enough from this point of view.

Some years ago, we suggested a new solution [57] for the mean spherical approximation (MSA) [58] for the square-well (SW) model. This solution, in conjunction with the linear trajectory approximation (LTA) [59,60], gives an opportunity to calculate the self-diffusion coefficients in pure liquid metals and in their binary alloys.

Recently, we successfully applied the SW-MSA-LTA approach to study the self-diffusivities in liquid binary alloys of alkali metals [61] and in liquid pure noble metals [62]. Here, we apply this approach for the same aim to liquid Cu-Ag, Cu-Au, and Ag-Au alloys. The chosen alloys have different types of phase diagrams in spite of the similar electron structures of pure Cu, Ag, and Au. It makes the study of these alloys interesting from the point of view of investigating which one from these factors has more influence on their properties. On the other hand, due to the high resistance to the chemical activity as well as the high electro- and heat-conductivities, the alloys of noble metals are widely used in

the industry. Moreover, Au-Ag and Au-Cu are jewelry alloys, for manufacturing of which it is necessary to know the velocity of the concentrations' convergence at melting, which depends on the diffusion properties.

2. Theory

In accordance with Einstein's well-known expression [63], the self-diffusion coefficient of the i -th-kind atom in the mixture D_i is inversely proportional to the friction coefficient of the same atom, ξ_i :

$$D_i = (\beta \xi_i)^{-1} \quad (1)$$

where $\beta = (k_B T)^{-1}$; k_B is the Boltzmann constant; T is the temperature.

In the LTA suggested by Helfand [59] for pure fluids described by the hard-core (HC) pair potentials,

$$\xi = \xi_{\text{HC}} + \xi_{\text{non-HC}} \quad (2)$$

where ξ_{HC} is the hard-core part of the pair interaction [64]; $\xi_{\text{non-HC}}$ is the contribution to the friction coefficient caused by the non-hard-core part of the pair interaction:

$$\xi_{\text{HC}} = \frac{8}{3} \rho \sigma^2 g(\sigma) (\pi M / \beta)^{1/2} \quad (3)$$

$$\xi_{\text{non-HC}} = -\frac{(\beta \pi M)^{1/2}}{12\pi^2} \int_0^\infty [S(q) - 1] \phi(q) q^3 dq \quad (4)$$

Here, ρ is the mean atomic density; σ is the diameter of the hard core; $g(r)$ is the pair correlation function; M is the atomic mass; $S(q)$ is the structure factor; $\phi(q)$ is the Fourier transform of the pair potential, $\phi(r)$, outside the hard core.

Davis and Palyvos [60] modified Equation (2) by taking into account the cross effect between HC and non-HC forces, and generalized the resulting expression to γ -component mixtures:

$$\xi_i = \xi_i^{\text{HC}} + \xi_i^{\text{non-HC}} + \xi_i^{\text{cross}} \quad (5)$$

where

$$\xi_i^{\text{HC}} = \frac{8}{3} (2\pi/\beta)^{1/2} \sum_{j=1}^{\gamma} \rho_j \sigma_{ij}^2 g_{ij}(\sigma_{ij}) \mu_{ij}^{1/2} \quad (6)$$

$$\xi_i^{\text{non-HC}} = -\frac{(2\pi\beta)^{1/2}}{12\pi^2} \sum_{j=1}^{\gamma} \rho_j \mu_{ij}^{1/2} \int_0^\infty h_{ij}(q) \phi_{ij}(q) q^3 dq \quad (7)$$

$$\xi_i^{\text{cross}} = -\frac{(2\beta/\pi)^{1/2}}{3} \sum_{j=1}^{\gamma} \rho_j \mu_{ij}^{1/2} g_{ij}(\sigma_{ij}) \int_0^\infty (x_{ij} \cos(x_{ij}) - \sin(x_{ij})) \phi_{ij}(q) dq \quad (8)$$

Here, $\rho_i = c_i \rho$; c_i is the concentration of the i -th component; σ_{ij} is the partial HC diameter; $g_{ij}(r)$ is the partial pair correlation function; $\mu_{ij} = M_i M_j / (M_i + M_j)$; M_i is the atomic mass of the i -th component; $h_{ij}(q)$ is the Fourier transform of $(g_{ij}(r) - 1)$; and $\phi_{ij}(q)$ is the Fourier transform of the partial pair potential, $\phi_{ij}(r)$, at $r \geq \sigma_{ij}$; $x_{ij} = q\sigma_{ij}$.

For the SW binary mixture, Equations (6)–(8) are being rewritten as

$$\xi_i^{\text{HC}} = \frac{8}{3} (2\pi/\beta)^{1/2} \sum_{j=1}^2 \rho_j \sigma_{ij}^2 g_{ij}^{\text{SW}}(\sigma_{ij}) \mu_{ij}^{1/2} \quad (9)$$

$$\xi_i^{\text{non-HC}} = -\frac{(2\pi\beta)^{1/2}}{12\pi^2} \sum_{j=1}^2 \sqrt{\frac{c_j}{c_i}} \mu_{ij}^{1/2} \int_0^\infty \left(S_{ij}^{\text{SW}}(q) - \delta_{ij} \right) \phi_{ij}^{\text{SW}}(q) q^3 dq \quad (10)$$

$$\xi_i^{\text{cross}} = -\frac{(2\beta/\pi)^{1/2}}{3} \sum_{j=1}^2 \rho_j \mu_{ij}^{1/2} g_{ij}^{\text{SW}}(\sigma_{ij}) \int_0^\infty (x_{ij} \cos(x_{ij}) - \sin(x_{ij})) \phi_{ij}^{\text{SW}}(q) dq \quad (11)$$

where

$$\delta_{ij} = \begin{cases} 1, & i = j \\ 0, & i \neq j \end{cases} \quad (12)$$

$S_{ij}(q)$ is the Ashcroft-Langreth [65] partial structure factor:

$$S_{ii}(q) = \frac{1 - c_j \rho c_{jj}(q)}{[1 - c_1 \rho c_{11}(q)][1 - c_2 \rho c_{22}(q)] - c_1 c_2 \rho^2 c_{12}^2(q)} \quad (13)$$

$$S_{12}(q) = \frac{\sqrt{c_1 c_2} \rho c_{12}(q)}{[1 - c_1 \rho c_{11}(q)][1 - c_2 \rho c_{22}(q)] - c_1 c_2 \rho^2 c_{12}^2(q)} \quad (14)$$

where $i \neq j$; $c_{ij}(q)$ is the Fourier transform of the partial direct correlation function, $c_{ij}(r)$;

$$\phi_{ij}^{\text{SW}}(q) = 4\pi \varepsilon_{ij} [\sin(\lambda_{ij} x_{ij}) - \sin(x_{ij}) - \lambda_{ij} x_{ij} \cos(\lambda_{ij} x_{ij}) + x_{ij} \cos(x_{ij})] / q^3 \quad (15)$$

where ε_{ij} is the partial SW depth and $(\lambda_{ij} - 1)\sigma_{ij}$ is the partial SW width. For the additive mixture exploited here, the Lorentz–Berthelot rule is used to describe parameters attributed to the unlike-atoms' interaction:

$$\begin{aligned} \sigma_{12} &= (\sigma_{11} + \sigma_{22})/2, \\ \varepsilon_{12} &= -\sqrt{\varepsilon_{11}\varepsilon_{22}}, \\ \lambda_{12} &= (\lambda_{11}\sigma_{11} + \lambda_{22}\sigma_{22})/(\sigma_{11} + \sigma_{22}). \end{aligned} \quad (16)$$

The Fourier transform of the partial direct correlation function is calculated here in the framework of the semi-analytical method [57] of solving the Ornstein–Zernike equation [66] for the square-well fluid within the mean spherical approximation [61,67,68]:

$$c_{ii}^{\text{SW}}(q) = -\beta \varphi_{ii}^{\text{SW}}(q) + \left(\frac{4\pi}{q^3}\right) \left\{ \sum_{m=1}^{n+2} x_{ii}^{2-m} \frac{\partial^m \sin(x_{ii})}{\partial x_{ii}^m} \sum_{l=0}^n b_{il} \prod_{k=0}^{m-2} (l+1-k) + \sum_{m=1}^{[(n+1)/2]} \frac{(-1)^{m+1} (2m)! b_{ii(2m-1)}}{x_{ii}^{2m-1}} \right\} \quad (17)$$

$$c_{12}^{\text{SW}}(q) = -\beta \varphi_{12}^{\text{SW}}(q) + \left(\frac{4\pi}{q^3}\right) \left\{ \sum_{m=1}^{n+2} x_{11}^{2-m} \frac{\partial^m \sin(x_{12})}{\partial x_{12}^m} \sum_{l=0}^n b_{12l} \prod_{k=0}^{m-2} (l+1-k) + y_{12} b_{120} \cos(x_{12}) + \sum_{m=1}^n \frac{(m+1)! b_{12m}}{x_{11}^m} \frac{\partial^m \sin(y_{12})}{\partial y_{12}^m} \right\} \quad (18)$$

where $n \geq 3$ (we take n equal to 5); $y_{12} = q(\sigma_{22} - \sigma_{11})/2$ at $\sigma_{22} > \sigma_{11}$; $[(n+1)/2]$ is the integral part of $(n+1)/2$; and b_{ijm} are coefficients determined numerically from the condition that the partial pair correlation functions must be equal to zero inside the HC:

$$g_{ij}(r) = 0, \quad r < \sigma_{ij} \quad (19)$$

where $i, j = 1, 2$.

The condition (19) is fulfilled numerically by the simplex method using the well-known Fourier-transform relation:

$$g_{ij}(r) = 1 + \frac{1}{2\pi^2 \rho \sqrt{c_i c_j}} \int_0^\infty [S_{ij}(q) - \delta_{ij}] \frac{\sin(qr)}{qr} q^2 dq \quad (20)$$

3. Results and Discussion

Self-diffusion coefficients of the components in liquid Cu-Ag, Cu-Au, and Ag-Au alloys at different compositions are studied at two temperatures ($T = 1423$ K and $T = 1573$ K) for which we have the obtained earlier [62] SW-parameters' values of all three pure metals forming the alloys under consideration. We use the experimental values of the required mean atomic densities of alloys under consideration taken from the work [69] for Cu-Ag

and Ag-Au systems and from the work [70] for Cu-Au system. Values of the SW parameters for the alloy's components (σ_{ii} , ε_{ii} , λ_{ii}) are taken to be the same as ones for the pure metals from the work [62].

The calculated concentration dependencies of the self-diffusion coefficients of alloys' components in Cu-Ag, Cu-Au, and Ag-Au alloys are shown in Figure 1, Figure 2, and Figure 3, respectively. For the convenience of the readers, all obtained results are duplicated in Tables 1–3.

Table 1. Self-diffusion coefficients of Cu and Ag in liquid Cu-Ag alloy at $T = 1423$ K and $T = 1573$ K.

T (K)	$D \times 10^9$ (m ² /s)	c_{Cu}					
		0	0.2	0.4	0.6	0.8	1
1423	Cu		3.52	3.545	3.58	3.625	3.71
	Ag	3.24	2.25	3.265	3.29	3.32	
1573	Cu		4.63	4.675	4.74	4.82	4.91
	Ag	4.41	4.435	4.46	4.49	4.53	

Table 2. Self-diffusion coefficients of Cu and Au in liquid Cu-Au alloy at $T = 1423$ K and $T = 1573$ K.

T (K)	$D \times 10^9$ (m ² /s)	c_{Cu}				
		0	0.25	0.5	0.75	1
1423	Cu		3.20	3.30	3.50	3.71
	Au	2.28	2.30	2.40	2.50	
1573	Cu		4.38	4.50	4.64	4.91
	Au	3.08	3.15	3.27	3.40	

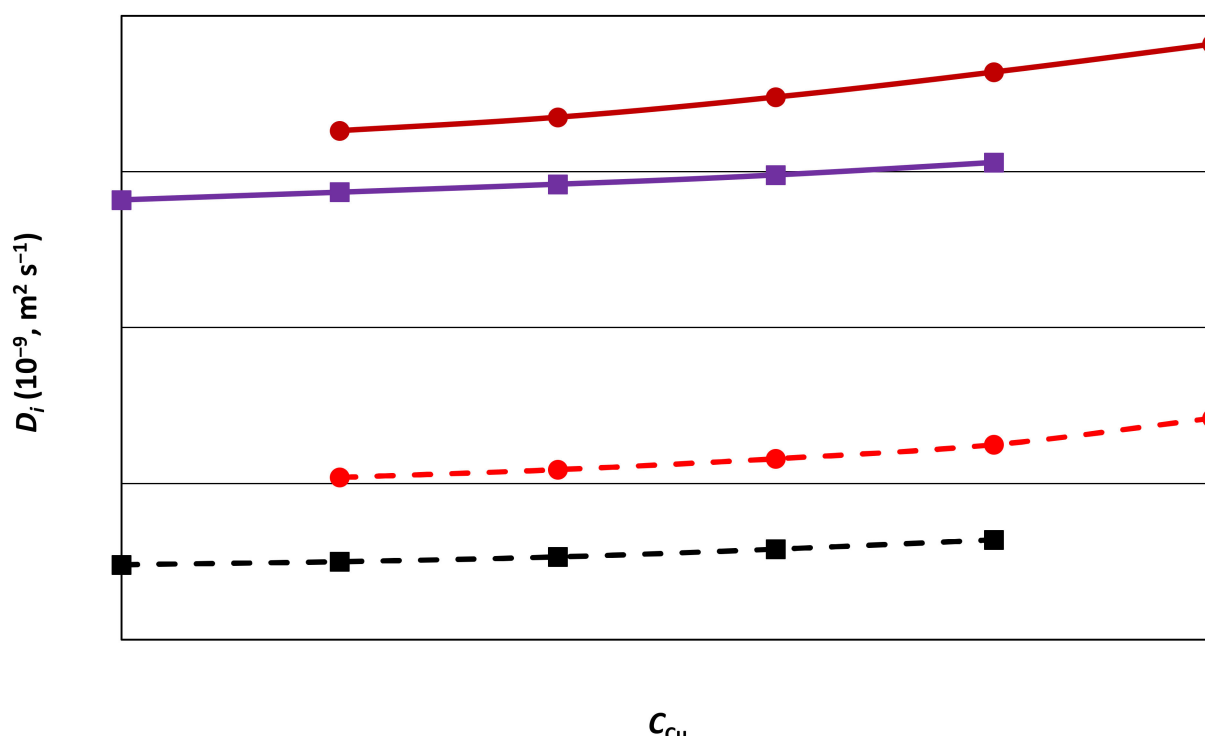


Figure 1. Self-diffusion coefficients of Cu (circles) and Ag (squares) in liquid Cu-Ag alloy at $T = 1423$ K (dashed line) and $T = 1573$ K (solid line).

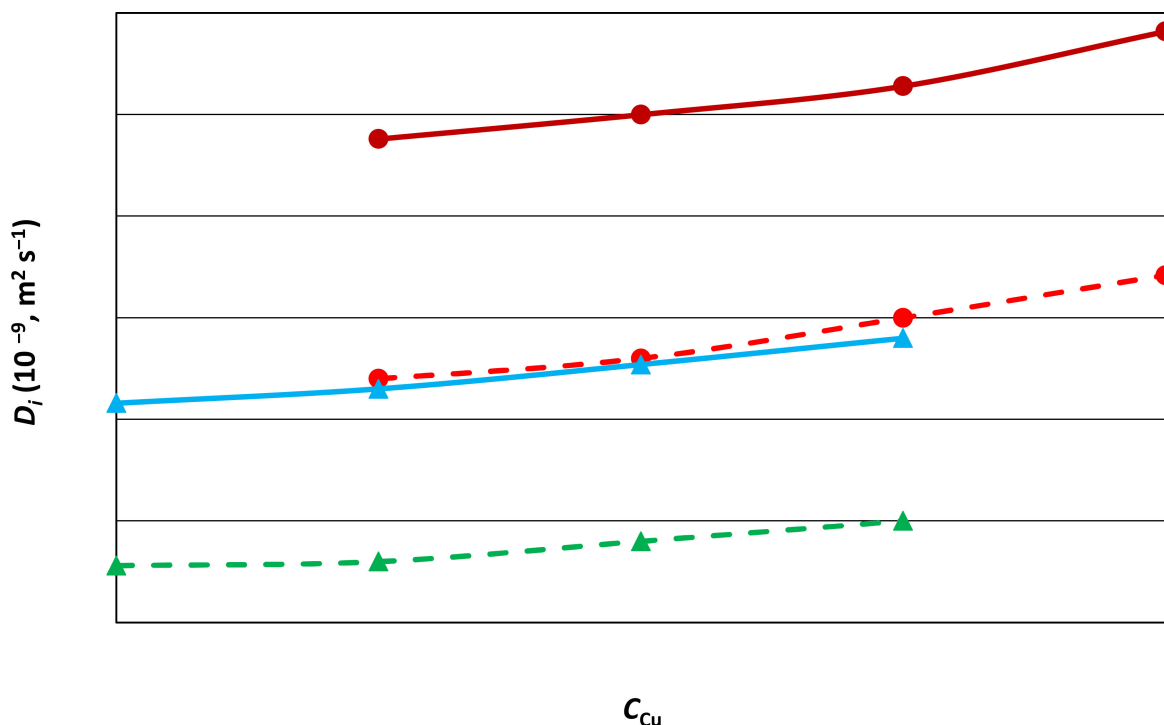


Figure 2. Self-diffusion coefficients of Cu (circles) and Au (triangles) in liquid Cu-Au alloy at $T = 1423 \text{ K}$ (dashed line) and $T = 1573 \text{ K}$ (solid line).

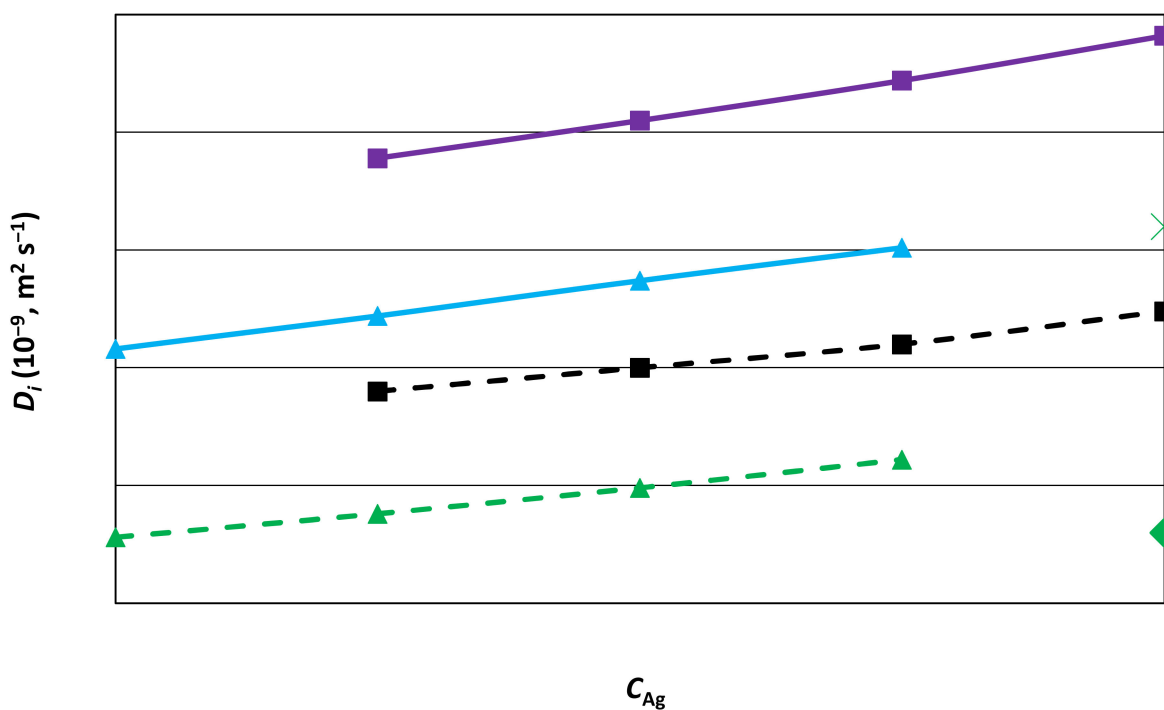


Figure 3. Self-diffusion coefficients of Ag (squares) and Au (triangles) in liquid Ag-Au alloy at $T = 1423 \text{ K}$ (dashed line) and $T = 1573 \text{ K}$ (solid line) in comparison with the self-diffusion coefficients of Au in pure Ag at $T = 1300 \text{ K}$ (rhombus) and at $T = 1500 \text{ K}$ (asterisk) taken from the experiment [71].

Table 3. Self-diffusion coefficients of Ag and Au in liquid Ag-Au alloy at $T = 1423$ K and $T = 1573$ K.

T (K)	$D \times 10^9$ (m^2/s)	c_{Ag}			
		0	0.25	0.5	0.75
1423	Ag		2.90	3.00	3.10
	Au	2.28	2.38	2.49	2.61
1573	Ag		3.89	4.05	4.22
	Au	3.08	3.22	3.37	3.51

Unfortunately, the experimental information needed for the comparison with obtained results is absent for the alloys under consideration. Therefore, we calculated the self-diffusion coefficients of Cu and Au in two Al-rich binary alloys with 20% of Cu and Au, respectively, at the same temperatures as we take for Cu-Ag, Cu-Au, and Ag-Au alloys, to estimate the accuracy of our results in comparison with available literary information [7,51]. To realize these calculations, we used the experimental values of the mean atomic densities of $\text{Al}_{80}\text{-Cu}_{20}$ and $\text{Al}_{80}\text{-Au}_{20}$ alloys taken from the works [51,72], respectively. The obtained results listed in Table 4 agree well with both experimental data [7] and the results of classical molecular-dynamic (MD) simulations [51]. Note that the range of the experimental error in the work [7] (as it was reported in Figure 4 of the work [9]) is equal to approximately 8.5%. On the other hand, the uncertainty in determination of values for the SW parameters in our work can spread up to 4% in dependence on the kind of the parameter and the kind of the element. This leads to a calculation error for the self-diffusion coefficients in the range of approximately 8%. These facts show that our calculated results and experimental results [7] lie within the limits of the mutual error. For the results of the work [51], the range of the simulation error is not presented, and we can conclude only that the named results lie in the limits of our error.

Table 4. Self-diffusion coefficients of Cu and Au in liquid $\text{Al}_{80}\text{-Cu}_{20}$ and $\text{Al}_{80}\text{-Au}_{20}$ alloys, respectively, at $T = 1423$ K and $T = 1573$ K calculated in the present work in comparison with the experimental [7] and MD-simulation [51] results for $\text{Al}_{80}\text{-Cu}_{20}$ and $\text{Al}_{80}\text{-Au}_{20}$ alloys, respectively.

$D \times 10^9$ (m^2/s)	T (K)	Our Results	Literature Results
Cu	1423	7.95	7.86 [7]
	1573	10.47	10.28 [7]
Au	1423	2.50	2.41 [51]
	1573	3.43	3.10 [51]

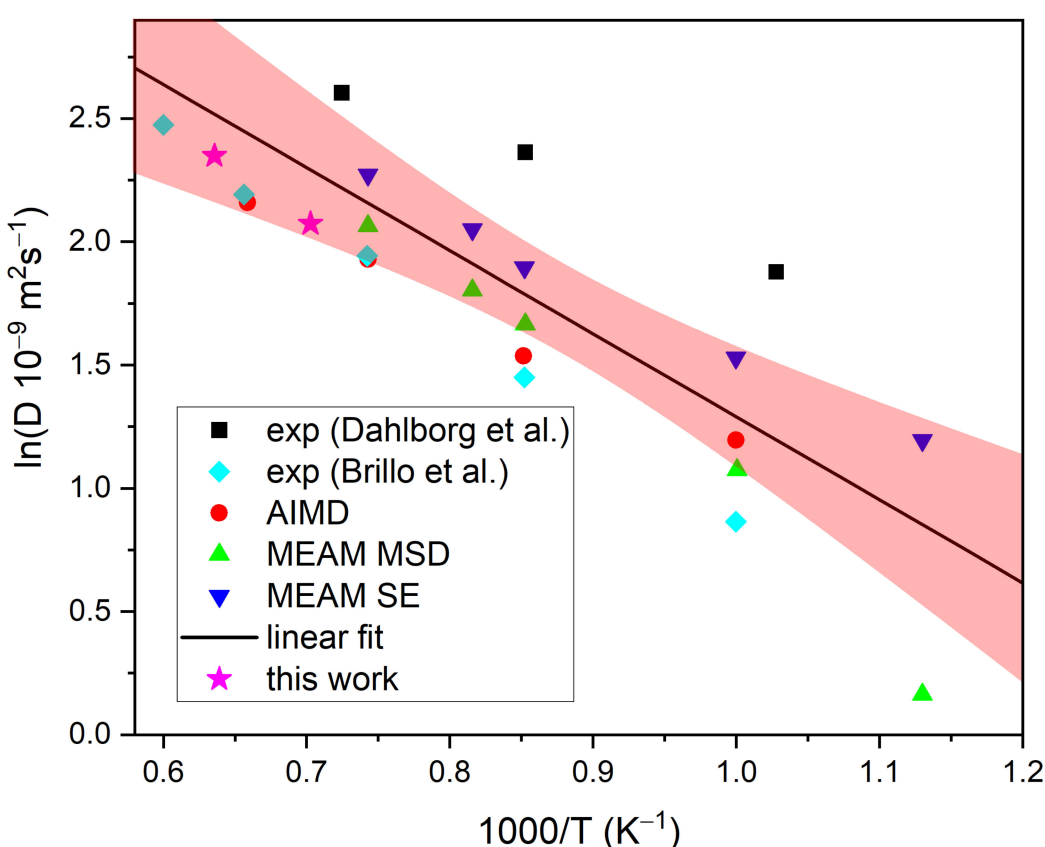


Figure 4. Arrhenius plot of the self-diffusivity of Cu in Al₈₀-Cu₂₀ liquid alloy obtained by different methods [7,15,73,74] in comparison with our results (the red area restricts the 95% confidence interval of the linear fit).

As far as we know, there has only been work carried out [51] where self-diffusivities of Au in Al-Au liquid alloy were studied. At the same time, for Al₈₀-Cu₂₀ melt, there are several available sources with data on the self-diffusivities of Cu at different temperatures: experimental data of Brillo et al. [7] and Dahlborg et al. [15], results of ab initio molecular dynamics (AIMD) obtained by Wang et al. [73], and results of classical MD simulations with modified embedded atom model (MEAM) obtained by Trybula [74], who used both the mean square displacement (MSD) and the Stokes-Einstein (SE) equation. To estimate the accuracy of our results more correctly, the statistical analysis of the named above data was performed as follows: all these data were collected together and fitted by linear function, after which the 95% confidence interval of the fit was calculated and compared with our calculations (Figure 4). One can see that our data are within the obtained confidence interval.

Thus, this additional study and our earlier results on the self-diffusivities of liquid Cu, Ag, and Au in the pure state [62] show a satisfactory agreement of the calculated results with the ones in the literature, and allow us to hope for the high reliability of the results for Cu-Ag, Cu-Au, and Ag-Au presented in Figures 1–3.

From Figures 1–3, one can see that the behavior of the concentration dependencies of the self-diffusion coefficients is slightly different for all three systems. In Ag-Au system, having the full mutual solubility of components in the solid state, these dependencies are the straight lines (Figure 3). In the Cu-Ag eutectic system, some concavities are observed on all calculated curves (Figure 1). In the Cu-Au system, all obtained curves are slightly fractured and, herewith, the positions of the bends correspond approximately to the alloy's compositions at which the chemical compounds exist in this system in the solid state at low temperatures (Figure 2).

The comparison of the results obtained at different temperatures show that the changing of the temperature leads to a significant change in magnitude of the self-diffusivity, but has almost no effect on the behavior of the concentration dependencies under consideration.

In Figure 3, the experimental self-diffusion coefficients of Au in pure Ag at $T = 1300$ K and at $T = 1500$ K [71] are shown. It can be seen that our results are slightly understated in comparison with this experiment.

4. Conclusions

This work shows that the SW-MSA-LTA approach allows the obtaining of satisfactory results for the diffusion coefficient in liquid binary alloys of noble metals as well as for the liquid binary alloys of alkali metals, as it was shown earlier [61].

Since the experimental data for the objects under study are absent, the results obtained can be used for an approximate estimation, encouraging experimental or MD-simulation studies of the systems under consideration.

Author Contributions: N.D. and R.R. provided methodology and wrote the manuscript; N.D. provided the calculations for alloys of noble metals; R.R. provided the calculations for Al-rich binary alloys. All authors have read and agreed to the published version of the manuscript.

Funding: This study was funded by the Russian Science Foundation, Grant № 22-22-00506, <https://rscf.ru/project/22-22-00506/> (accessed on 11 January 2021).

Institutional Review Board Statement: Not applicable.

Informed Consent Statement: Not applicable.

Data Availability Statement: Data are contained within the article.

Acknowledgments: The numerical calculations are carried out using computational resources of the “Uran” supercomputer of IMM UB RAS (<http://parallel.uran.ru> (accessed on 11 January 2021)) and Joint Supercomputer Center of Russian Academy of Sciences (<http://www.jsc.ru> (accessed on 1 January 2022)).

Conflicts of Interest: The authors declare no conflict of interest.

References

1. Feinauer, A.; Majer, G. Diffusion of ^{23}Na and ^{39}K in the eutectic melt $\text{Na}_{0.32}\text{K}_{0.68}$. *Phys. Rev. B* **2001**, *64*, 134302. [[CrossRef](#)]
2. Lee, J.H.; Liu, S.; Miyahara, H.; Trivedi, R. Diffusion-coefficient measurements in liquid metallic alloys. *Metall. Mater. Trans. B* **2004**, *35*, 909–917. [[CrossRef](#)]
3. Das, S.K.; Horbach, J.; Koza, M.M.; Chatoh, S.M.; Meyer, A. Influence of chemical short-range order on atomic diffusion in Al–Ni melts. *Appl. Phys. Lett.* **2005**, *86*, 011918. [[CrossRef](#)]
4. Tanaka, Y.; Kajihara, M. Evaluation of interdiffusion in liquid phase during reactive diffusion between Cu and Al. *Mater. Trans.* **2006**, *47*, 2480–2488. [[CrossRef](#)]
5. Horbach, J.; Das, S.K.; Griesche, A.; Frohberg, G.; Macht, M.-P.; Meyer, A. Self-diffusion and interdiffusion in Al₈₀Ni₂₀ melts: Simulation and experiment. *Phys. Rev. B* **2007**, *75*, 174304. [[CrossRef](#)]
6. Kehr, M.; Schick, M.; Hoyer, W.; Egry, I. Viscosity of the binary system Al–Ni. *High Temp. High Press.* **2008**, *37*, 361–369.
7. Brillo, J.; Chathoth, S.M.; Koza, M.M.; Meyer, A. Liquid Al₈₀Cu₂₀: Atomic diffusion and viscosity. *Appl. Phys. Lett.* **2008**, *93*, 121905. [[CrossRef](#)]
8. Holland-Moritz, D.; Stüber, S.; Hartmann, H.; Unruh, T.; Hansen, T.; Meyer, A. Structure and dynamics of liquid Ni₃₆Zr₆₄ studied by neutron scattering. *Phys. Rev. B* **2009**, *79*, 064204. [[CrossRef](#)]
9. Zhang, B.; Griesche, A.; Meyer, A. Diffusion in Al–Cu Melts Studied by Time-Resolved X-ray Radiography. *Phys. Rev. Lett.* **2010**, *104*, 035902. [[CrossRef](#)]
10. Stüber, S.; Holland-Moritz, D.; Unruh, T.; Meyer, A. Ni self-diffusion in refractory Al–Ni melts. *Phys. Rev. B* **2010**, *81*, 024204. [[CrossRef](#)]
11. Brillo, J.; Pommrich, I.; Meyer, A. Relation between self-diffusion and viscosity in dense liquids: New experimental results from electrostatic levitation. *Phys. Rev. Lett.* **2011**, *107*, 165902. [[CrossRef](#)]
12. Lee, N.; Cahoon, J. Interdiffusion of copper and iron in liquid aluminum. *J. Phase Equilibr. Diffus.* **2011**, *32*, 226–234. [[CrossRef](#)]
13. Wu, S.; Kramer, M.J.; Fang, X.W.; Wang, S.Y.; Wang, C.Z.; Ho, K.M.; Ding, J.; Chen, L.Y. Structural and dynamical properties of liquid Cu₈₀Si₂₀ alloy studied experimentally and by ab initio molecular dynamics simulations. *Phys. Rev. B* **2011**, *84*, 134208. [[CrossRef](#)]

14. Kargl, F.; Sondermann, E.; Weis, H.; Meyer, A. Impact of convective flow on long-capillary chemical diffusion studies of liquid binary alloys. *High Temp. High Press.* **2013**, *42*, 3–21.
15. Dahlborg, U.; Besser, M.; Kramer, M.J.; Morris, J.R.; Calvo-Dahlborg, M. Atomic dynamics in molten AlCu alloys of different compositions and at different temperatures by cold neutron scattering. *Phys. B* **2013**, *412*, 50–60. [[CrossRef](#)]
16. Geng, Y.; Zhu, C.; Zhang, B. A sliding cell technique for diffusion measurements in liquid metals. *AIP Adv.* **2014**, *4*, 037102. [[CrossRef](#)]
17. Engelhardt, M.; Meyer, A.; Yang, F.; Simeoni, G.G.; Kargl, F. Self and chemical diffusion in liquid Al-Ag. *Def. Diff. Forum* **2016**, *367*, 157–166. [[CrossRef](#)]
18. Zhong, L.; Hu, J.; Geng, Y.; Zhu, C.; Zhang, B. A multi-slice sliding cell technique for diffusion measurements in liquid metals. *Rev. Sci. Instrum.* **2017**, *88*, 093905. [[CrossRef](#)]
19. Xiong, L.H.; Wang, X.D.; Cao, Q.P.; Zhang, D.X.; Xie, H.L.; Xiao, T.Q.; Jiang, J.Z. Composition- and temperature-dependent liquid structures in Al-Cu alloys: An ab initio molecular dynamics and x-ray diffraction study. *J. Phys. Condens. Matter* **2017**, *29*, 035101. [[CrossRef](#)]
20. Belova, I.V.; Heuskin, D.; Sondermann, E.; Ignatzi, B.; Kargl, F.; Murch, G.E.; Meyer, A. Combined interdiffusion and self-diffusion analysis in Al-Cu liquid diffusion couple. *Scr. Mater.* **2018**, *143*, 40–43. [[CrossRef](#)]
21. Sondermann, E.; Jakse, N.; Binder, K.; Mielke, A.; Heuskin, D.; Kargl, F.; Meyer, A. Concentration dependence of interdiffusion in aluminum-rich Al-Cu melts. *Phys. Rev. B* **2019**, *99*, 024204. [[CrossRef](#)]
22. Baumketner, A.; Chushak, Y. A molecular dynamics study of the diffusion processes in liquid Na-K alloys. *J. Phys. Condens. Matter* **1999**, *11*, 1397–1408. [[CrossRef](#)]
23. Genser, O.; Hafner, J. Structure and bonding in crystalline and molten Li-Sn alloys: A first-principles density-functional study. *Phys. Rev. B* **2001**, *63*, 144204. [[CrossRef](#)]
24. Gonzalez, D.J.; Gonzalez, L.E.; Lopez, J.M.; Stott, M.J. Atomic dynamics in simple liquid metals and alloys. *J. Non-Cryst. Solids* **2002**, *314*, 110–120. [[CrossRef](#)]
25. Bhuiyan, G.M.; Ali, I.; Rahman, S.M.M. Atomic transport properties of AgIn liquid binary alloys. *Phys. B* **2003**, *334*, 147–159. [[CrossRef](#)]
26. Bailey, N.P. Simulation of Cu-Mg metallic glass: Thermodynamics and structure. *Phys. Rev. B* **2004**, *69*, 144205. [[CrossRef](#)]
27. Gonzalez, D.J.; Gonzalez, L.E.; Lopez, J.M.; Stott, M.J. Microscopic dynamics in the liquid Li-Na alloy: An ab initio molecular dynamics study. *Phys. Rev. E* **2004**, *69*, 031205. [[CrossRef](#)]
28. Wang, S.; Wang, C.Z.; Chuang, F.; Morris, J.R.; Ho, K.M. Ab initio molecular dynamics simulation of liquid Al₈₈Si₁₂ alloys. *J. Chem. Phys.* **2005**, *122*, 034508. [[CrossRef](#)]
29. Zhao, G.; Liu, C.S.; Zhu, Z.G. Ab initio molecular-dynamics simulations of the structural properties of liquid In₂₀Sn₈₀ in the temperature range 798–1193 K. *Phys. Rev. B* **2006**, *73*, 024201. [[CrossRef](#)]
30. Wax, J.F.; Jakse, N. Large-scale molecular dynamics study of liquid K-Cs alloys: Structural, thermodynamic, and diffusion properties. *Phys. Rev. B* **2007**, *75*, 0242004. [[CrossRef](#)]
31. Dalgic, S.S.; Sengul, S. Structure and atomic transport properties in liquid AsTe alloys using AMEAM based potentials. *J. Optoelectr. Adv. Mater.* **2007**, *9*, 1699–1704.
32. Dalgic, S.S.; Celtek, M.; Dalgic, S. Effective pair potentials for molten Cu-Ge alloys. *J. Optoelectr. Adv. Mater.* **2007**, *9*, 1710–1714.
33. Bhuiyan, E.H.; Ahmed, A.Z.Z.; Bhuiyan, G.M.; Shahjahan, M. Atomic transport properties of Ag_xSn_{1-x} liquid binary alloys. *Phys. B* **2008**, *403*, 1695–1703. [[CrossRef](#)]
34. Das, S.K.; Horbach, J.; Thomas, V. Structural relaxation in a binary metallic melt: Molecular dynamics computer simulation of undercooled Al₈₀Ni₂₀. *Phys. Rev. B* **2008**, *78*, 064208. [[CrossRef](#)]
35. Cheng, H.; Lü, Y.J.; Chen, M. Interdiffusion in liquid Al-Cu and Ni-Cu alloys. *J. Chem. Phys.* **2009**, *131*, 044502. [[CrossRef](#)] [[PubMed](#)]
36. Wang, S.Y.; Kramer, M.J.; Xu, M.; Wu, S.; Hao, S.G.; Sordelet, D.J.; Ho, K.M.; Wang, C.Z. Experimental and ab initio molecular dynamics simulation studies of liquid Al₆₀Cu₄₀ alloy. *Phys. Rev. B* **2009**, *79*, 144205. [[CrossRef](#)]
37. Wang, S.; Wang, C.Z.; Zheng, C.X.; Ho, K.M. Structure and dynamics of liquid Al_{1-x}Si_x alloys by ab initio molecular dynamics simulations. *J. Non-Cryst. Solids* **2009**, *355*, 340–347. [[CrossRef](#)]
38. Zhu, X.F.; Chen, L.F. Ab initio molecular-dynamics simulation of liquid As_xTe_{1-x} alloys. *J. Phys. Condens. Matter* **2009**, *21*, 275602. [[CrossRef](#)]
39. Zhao, G.; Zhao, Y.; Wang, Y.; Ji, C. Ab initio molecular dynamics study of liquid Se₃₀Te₇₀: Structural, electronic and dynamical properties. *Phys. Scr.* **2010**, *82*, 035603. [[CrossRef](#)]
40. Pasturel, A.; Tascli, E.S.; Sluiter, M.H.F.; Jakse, N. Structural and dynamic evolution in liquid Au-Si eutectic alloy by ab initio molecular dynamics. *Phys. Rev. B* **2010**, *81*, 140202. [[CrossRef](#)]
41. Liu, D.; Qin, J.Y.; Gu, T.K. The structure of liquid Mg–Cu binary alloys. *J. Non-Cryst. Solids* **2010**, *356*, 1587–1592. [[CrossRef](#)]
42. Wax, J.-F.; Johnson, M.R.; Bove, L.E.; Mihalkovic, M. Multiscale study of the influence of chemical order on the properties of liquid Li-Bi alloys. *Phys. Rev. B* **2011**, *83*, 144203. [[CrossRef](#)]
43. Huang, L.; Wang, C.Z.; Ho, K.M. Structure and dynamics of liquid Ni₃₆Zr₆₄ by ab initio molecular dynamics. *Phys. Rev. B* **2011**, *83*, 184103. [[CrossRef](#)]

44. Han, X.J.; Schober, H.R. Transport properties and Stokes-Einstein relation in a computer-simulated glass-forming Cu33.3Zr66.7 melt. *Phys. Rev. B* **2011**, *83*, 224201. [[CrossRef](#)]
45. Ohmura, S.; Shimojo, F. Polymerization transition in liquid AsS under pressure: An ab initio molecular dynamics study. *Phys. Rev. B* **2011**, *84*, 224202. [[CrossRef](#)]
46. Souto, J.; Alemany, M.M.G.; Gallego, L.J.; González, L.E.; González, D.J. Static structure, microscopic dynamics and electronic properties of the liquid Bi–Pb alloy. An ab initio molecular dynamics study. *J. Nucl. Mater.* **2011**, *411*, 163–170. [[CrossRef](#)]
47. Qi, Y.; Wang, L.; Fang, T. Demixingbehaviour in binary Cu-Co melt. *Phys. Chem. Liq.* **2013**, *51*, 687–694. [[CrossRef](#)]
48. Cui, W.C.; Peng, C.X.; Wang, L.; Qi, Y.; Fang, T. Structure and dynamics of undercooled FeNi. *Phys. Chem. Liq.* **2014**, *52*, 88–99. [[CrossRef](#)]
49. Wang, N.; Jiang, T.; Yang, Y.; Tian, J.; Hu, S.; Peng, S.; Yan, L. Embedded atom model for the liquid U-10Zr alloy based on density functional theory calculations. *RSC Adv.* **2015**, *5*, 61495. [[CrossRef](#)]
50. Pasturel, A.; Jakse, N. On the role of entropy in determining transport properties in metallic melts. *J. Phys. Condens. Matter* **2015**, *27*, 325104. [[CrossRef](#)]
51. Peng, H.L.; Voigtman, T.; Kolland, G.; Kobatake, H.; Brillo, J. Structural and dynamical properties of liquid Al–Au alloys. *Phys. Rev. B* **2015**, *92*, 184201. [[CrossRef](#)]
52. Dziedzic, J.; Winczewski, S.; Rybicki, J. Structure and properties of liquid Al–Cu alloys: Empirical potentials compared. *Comput. Mater. Sci.* **2016**, *114*, 219–232. [[CrossRef](#)]
53. Pasturel, A.; Jakse, N. Validity of the Stokes–Einstein relation in liquids: Simple rules from the excess entropy. *J. Phys. Condens. Matter* **2016**, *28*, 485101. [[CrossRef](#)] [[PubMed](#)]
54. Cao, Q.; Wang, P.; Shao, J.; Wang, F. Transport properties and entropy-scaling laws for diffusion coefficients in liquid Fe0.9Ni0.1 up to 350 GPa. *RSC Adv.* **2016**, *6*, 84420. [[CrossRef](#)]
55. Yousefi, P.; Abbaspour, M.; Sokhanvaran, V. A comparative study of graphite and CNT supported Au–Ag, Au–Pd, Au–Pt and Au–Rh nanoalloys using MD simulation. *J. Mol. Liq.* **2019**, *280*, 87–96. [[CrossRef](#)]
56. Martínez, M.D.P.; Hoyuelos, M. From diffusion experiments to mean-field theory simulations and back. *J. Stat. Mech.* **2019**, *2019*, 113201. [[CrossRef](#)]
57. Dubinin, N.E.; Filippov, V.V.; Vatolin, N.A. Structure and thermodynamics of the one- and two-component square-well fluid. *J. Non-Cryst. Solids* **2007**, *353*, 1798–1801. [[CrossRef](#)]
58. Lebowitz, J.L.; Percus, J.K. Mean spherical model for lattice gases with extended hard cores and continuum fluids. *Phys. Rev.* **1966**, *144*, 251–258. [[CrossRef](#)]
59. Helfand, E. Theory of the molecular friction constant. *Phys. Fluids* **1961**, *4*, 681–691. [[CrossRef](#)]
60. Davis, H.T.; Palyvos, J.A. Contribution to the friction coefficient from time correlations between hard and soft molecular interactions. *J. Chem. Phys.* **1967**, *46*, 4043–4047. [[CrossRef](#)]
61. Dubinin, N.E. Square-well self-diffusion coefficients in liquid binary alloys of alkali metals within the mean spherical approximation. *J. Alloys Compd.* **2019**, *803*, 1100–1104. [[CrossRef](#)]
62. Dubinin, N.E. Self-diffusion in liquid copper, silver, and gold. *Metals* **2020**, *10*, 1651. [[CrossRef](#)]
63. Einstein, A. Über die von der molekularkinetischen theorie der wärme geforderte bewegung von in ruhenden flüssigkeiten suspendierten teilchen. *Ann. Phys.* **1905**, *322*, 549–560. [[CrossRef](#)]
64. Longuet-Higgins, H.C.; Valleau, J.P. Transport coefficients of dense fluids of molecules interacting according to a square well potential. *Mol. Phys.* **1958**, *1*, 284–294. [[CrossRef](#)]
65. Ashcroft, N.W.; Langreth, D.C. Structure of binary liquid mixtures. I. *Phys. Rev.* **1967**, *156*, 685–692. [[CrossRef](#)]
66. Ornstein, L.S.; Zernice, F. Interference of rontgen rays. *Proc. Natl. Acad. Sci. USA* **1914**, *17*, 793.
67. Dubinin, N.E.; Filippov, V.V.; Malkhanova, O.G.; Vatolin, N.A. Structure factors of binary liquid metal alloys within the square-well model. *Cent. Eur. J. Phys.* **2009**, *7*, 584–590. [[CrossRef](#)]
68. Dubinin, N.E.; Filippov, V.V.; Yuryev, A.A.; Vatolin, N.A. Excess entropy of mixing of binary square-well fluid in the mean spherical approximation: Application to liquid alkali-metal alloys. *J. Non-Cryst. Solids* **2014**, *401*, 101–104. [[CrossRef](#)]
69. Brillo, J.; Egry, I.; Ho, I. Density and thermal expansion of liquid Ag–Cu and Ag–Au alloys. *Int. J. Thermophys.* **2006**, *27*, 494–506. [[CrossRef](#)]
70. Brillo, J.; Egry, I.; Giffard, H.S.; Patti, A. Density and thermal expansion of liquid Au–Cu alloys. *Int. J. Thermophys.* **2004**, *25*, 1881–1888. [[CrossRef](#)]
71. Masaki, T.; Fukazawa, T.; Watanabe, Y.; Kaneko, M.; Yoda, S.; Itami, T. Measurement of diffusion coefficients of Au in liquid Ag with the shear cell technique. *J. Non-Cryst. Solids* **2007**, *353*, 3290–3294. [[CrossRef](#)]
72. Brillo, J.; Egry, I.; Westphal, J. Density and thermal expansion of liquid binary Al–Ag and Al–Cu alloys. *Int. J. Mat. Res.* **2008**, *99*, 162–167. [[CrossRef](#)]
73. Wang, W.Y.; Han, J.J.; Fang, H.Z.; Wang, J.; Liang, Y.F.; Shang, S.L.; Wang, Y.; Liu, X.J.; Kecskes, L.J.; Mathaudhu, S.N.; et al. Anomalous structural dynamics in liquid Al80Cu20: An ab initio molecular dynamics study. *Acta Mater.* **2015**, *97*, 75–85. [[CrossRef](#)]
74. Trybula, M.E. Structure and transport properties of the liquid Al80Cu20 alloy—A molecular dynamics study. *Comput. Mater. Sci.* **2016**, *122*, 341–352. [[CrossRef](#)]